Supplementary Information

Bisactinyl halogenated complexes: relativistic density functional theory calculation and experimental synthesis

Qing-Jiang Pan,*,† Yong-Ming Wang,† Run-Xue Wang,‡ Hong-Yue Wu,‡
Weiting Yang,‡ Zhong-Ming Sun,*,‡ Hong-Xing Zhang§

† Key Laboratory of Functional Inorganic Material Chemistry of Education Ministry, School of Chemistry and Materials Science, Heilongjiang University, Harbin 150080, China

‡ State Key Laboratory of Rare Earth Resource Utilization, Changchun Institute of Applied Chemistry, Chinese Academy of Sciences, Changchun, 130022, China

§ State Key Laboratory of Theoretical and Computational Chemistry, Institute of Theoretical Chemistry, Jilin University, Changchun 130023, China

*Corresponding authors: panqj@yahoo.com.cn (QJ Pan); szm@ciac.jl.cn (ZM Sun)

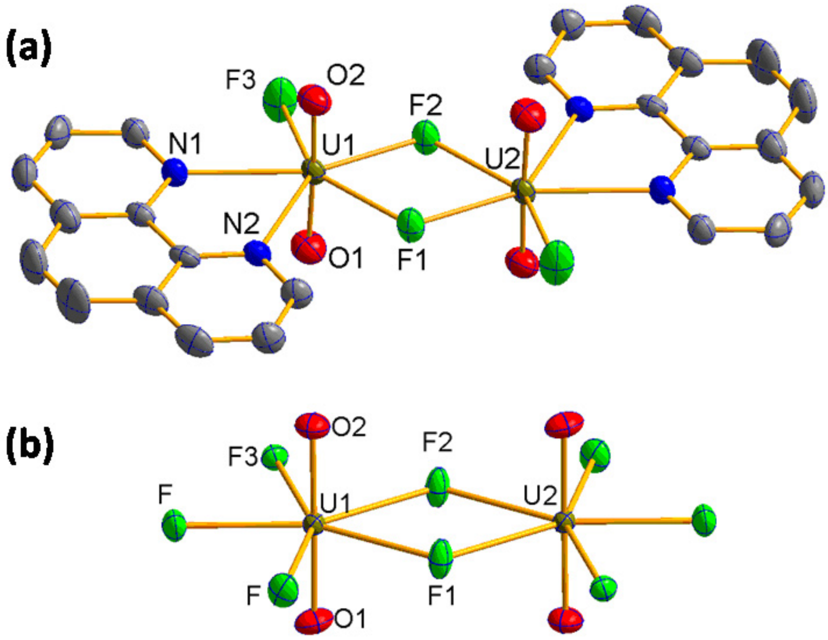

Figure S1. ORTEP representation of the asymmetric units of **1** (a) and **12** (b). Thermal ellipsoids are drawn at the 30 % probability level, and the hydrogen atoms are omitted for clarity.

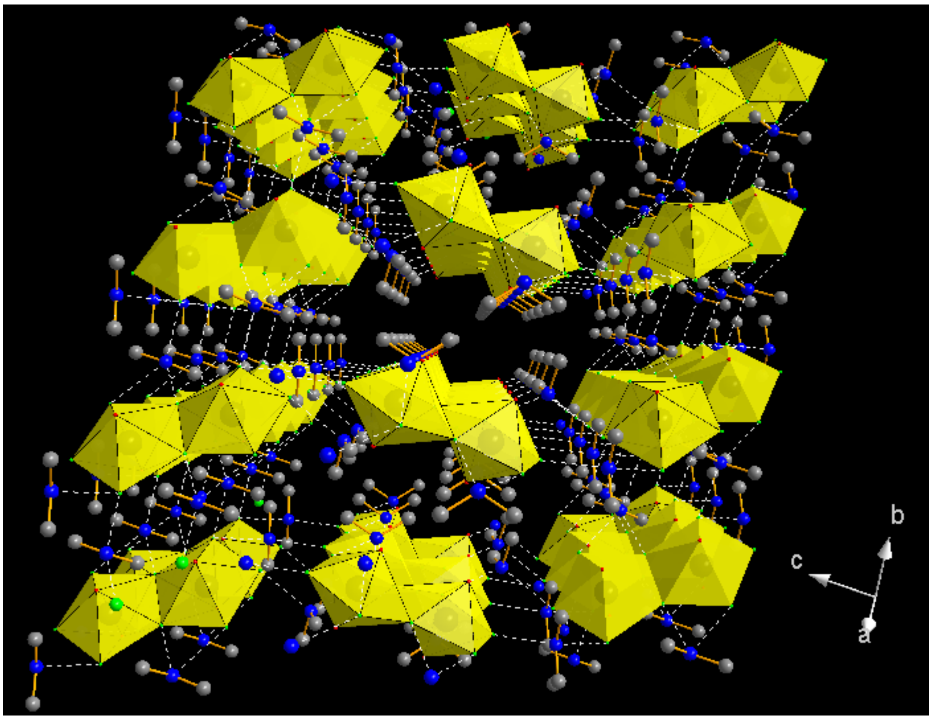

Figure S2. Representation of 3-D hydrogen-bonding interactions in complex **12** viewed along the <111> direction. N-H···F bonds are drawn as dashed white lines. Uranyl centered pentagonal bipyramids are represented as yellow polyhedra. Hydrogen atoms are omitted for clarity.

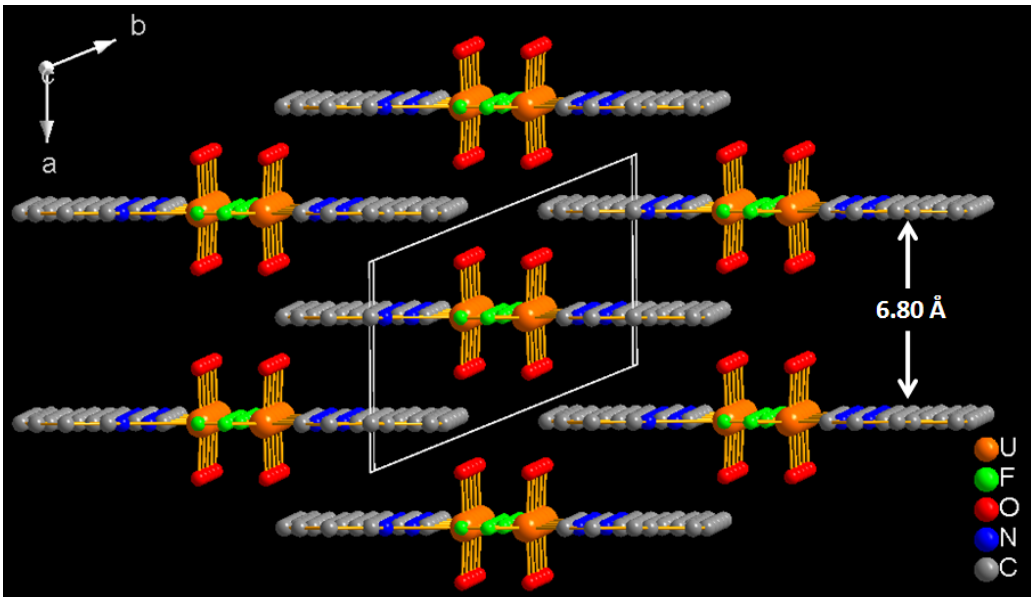

Figure S3. Structure of **1** viewed along the *c* axis. Hydrogen atoms are omitted for clarity.

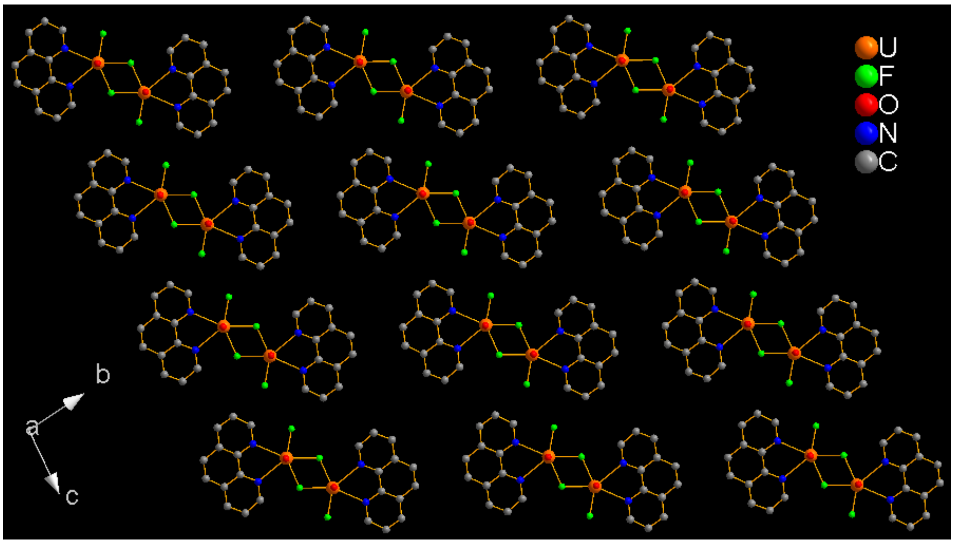

Figure S4. Layered distributions of **1** on the *bc* plane viewed along the *a* axis. Hydrogen atoms are omitted for clarity.

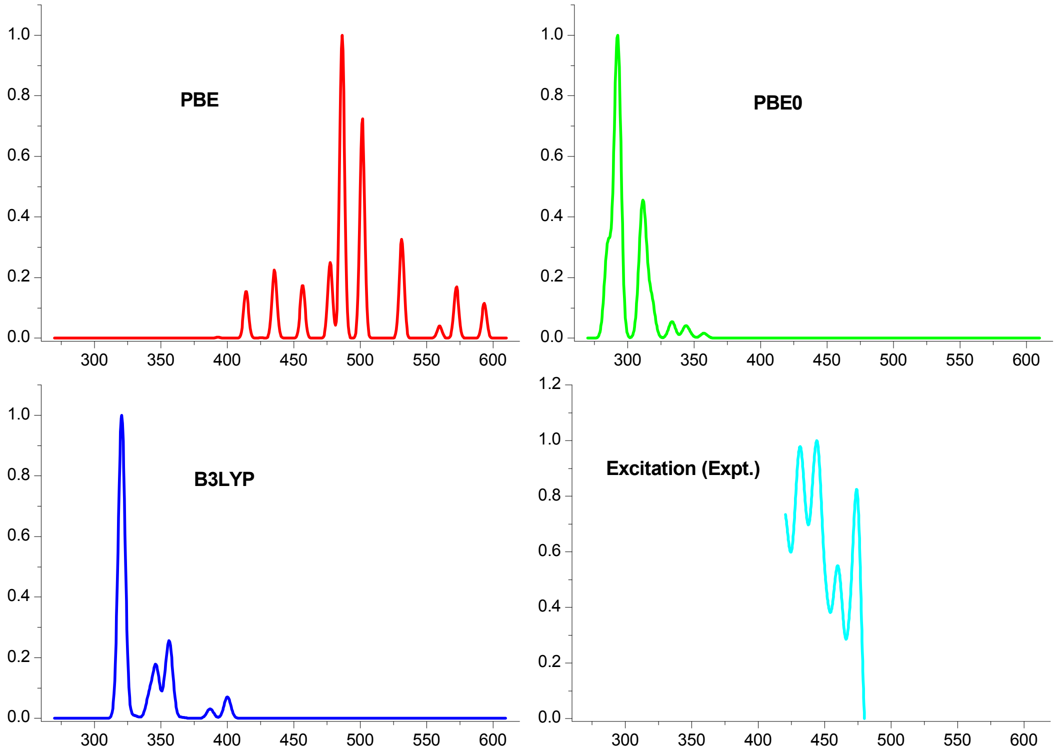

Figure S5. Simulated absorption spectra for **1** in water under the different density functional (GGA-PBE, Hybrid-PBE0 and Hybrid-B3LYP) calculations, compared with the experimentally obtained excitation spectra. For convenient comparison, all the spectra were normalized.

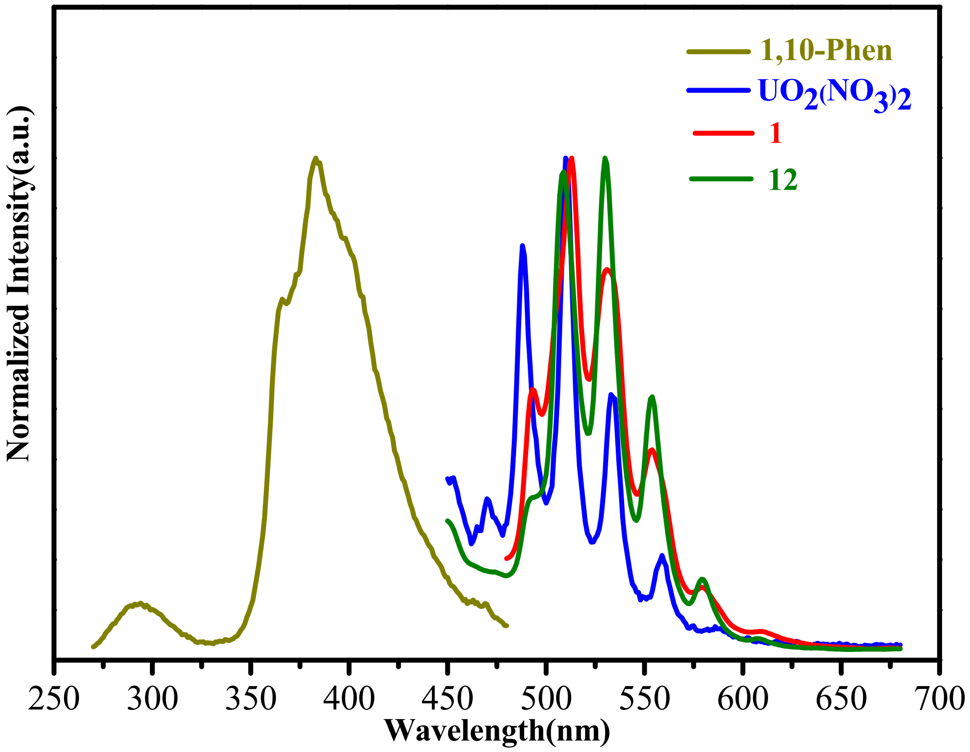

Figure S6. Fluorescent emission spectra of phenanthroline (Excited at 245 nm), $UO_2(NO_3)_2$, (at 428 nm) **1** and **12** (at 430 nm) in the solid state.

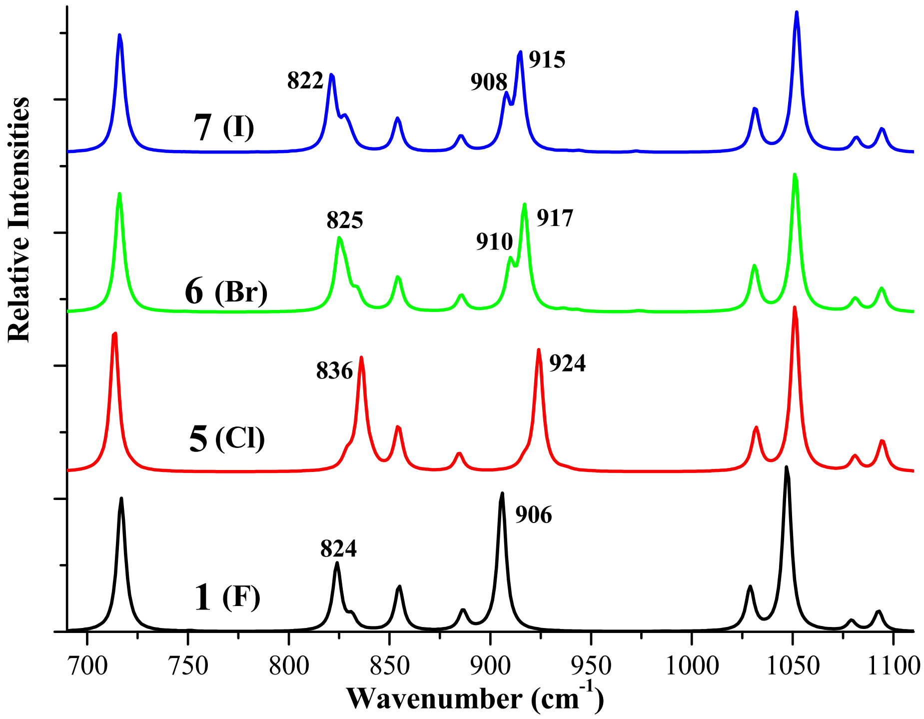

Figure S7. Simulated vibrational spectra of bisuranyl complexes, $[(phen)(UO_2)(\mu_2\text{-}X)(X)]_2$ (X = F (**1**), Cl (**5**), Br (**6**) and I (**7**)).

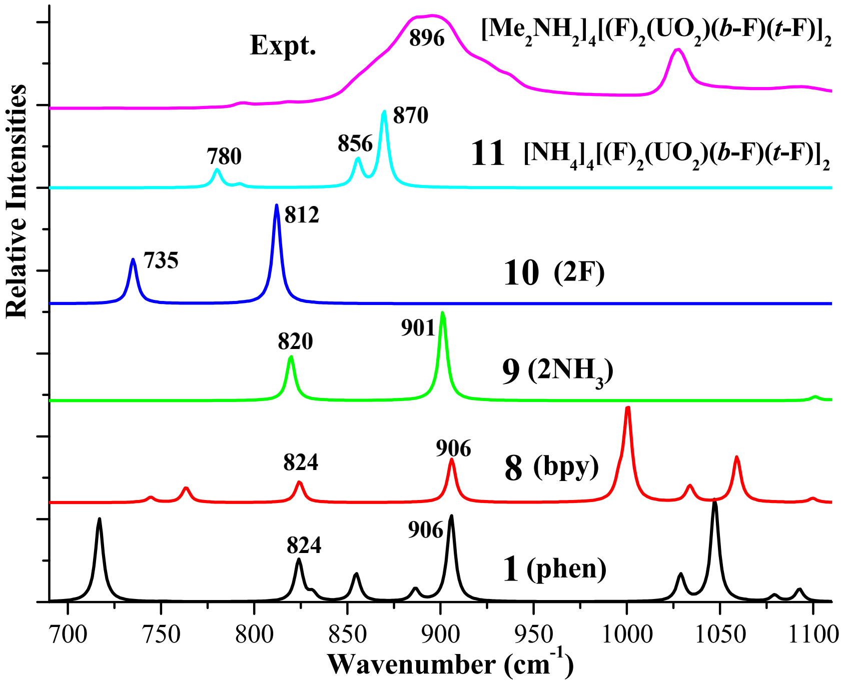

Figure S8. Simulated vibrational spectra of bisuranyl complexes, $[(L)(UO_2)(\mu_2\text{-}F)(F)]_2$ (L = phen (**1**), bpy (**8**), and $2NH_3$ (**9**)) and $[NH_4]_4[(F)_2(UO_2)(\mu_2\text{-}F)(F)]_2$ (**11**), together with experimental IR measurements of $[Me_2NH_2]_4[(F)_2(UO_2)(\mu_2\text{-}F)(F)]_2$ (**12**).

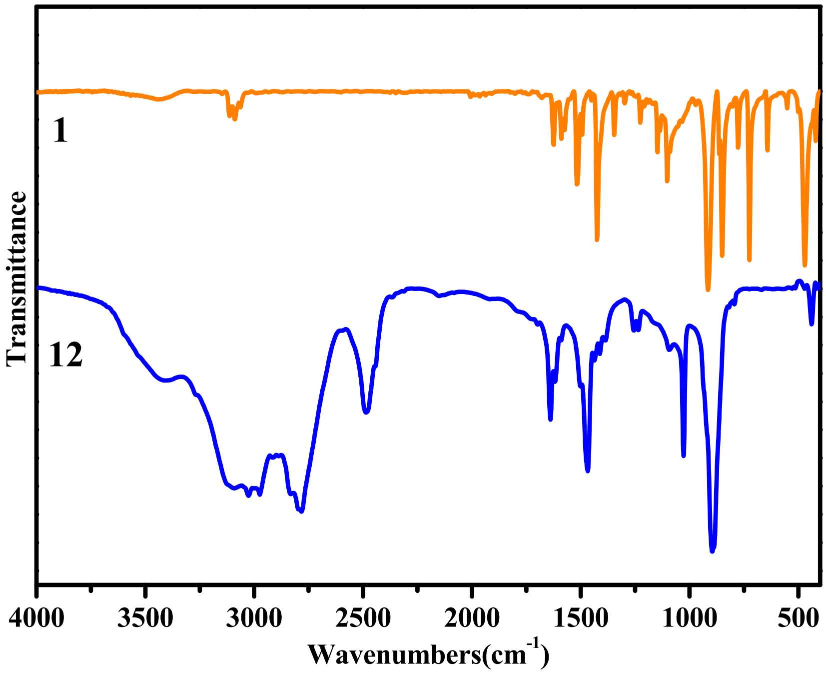

Figure S9. FTIR spectra of **1** and **12** measured as KBr pellets.

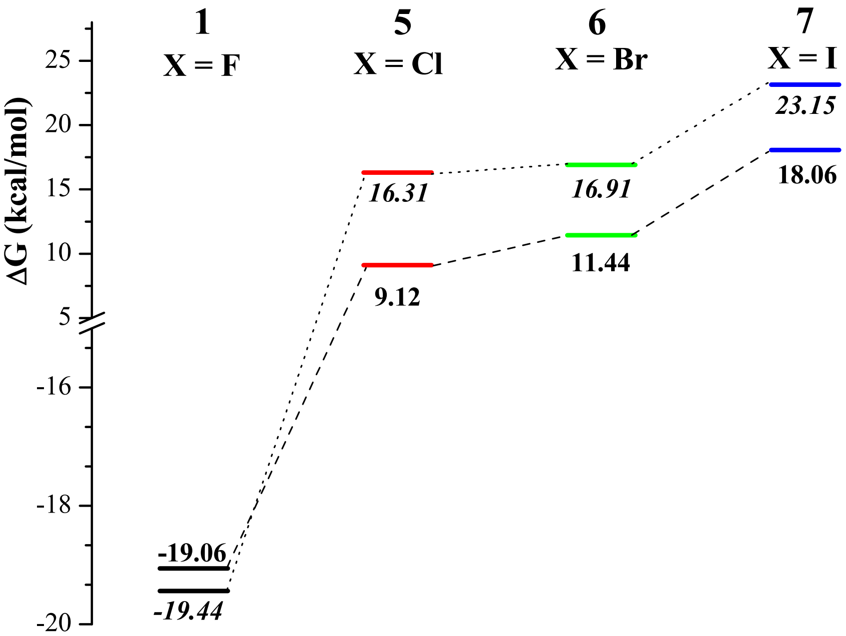

Figure S10. Free energies of formation reactions for bisuranyl complexes, [(phen)(UO_2)(μ_2-X)(X)]$_2$ (X = F (**1**), Cl (**5**), Br (**6**) and I (**7**)), in the gas phase (italic number) and aqueous solution (bold nubmer).

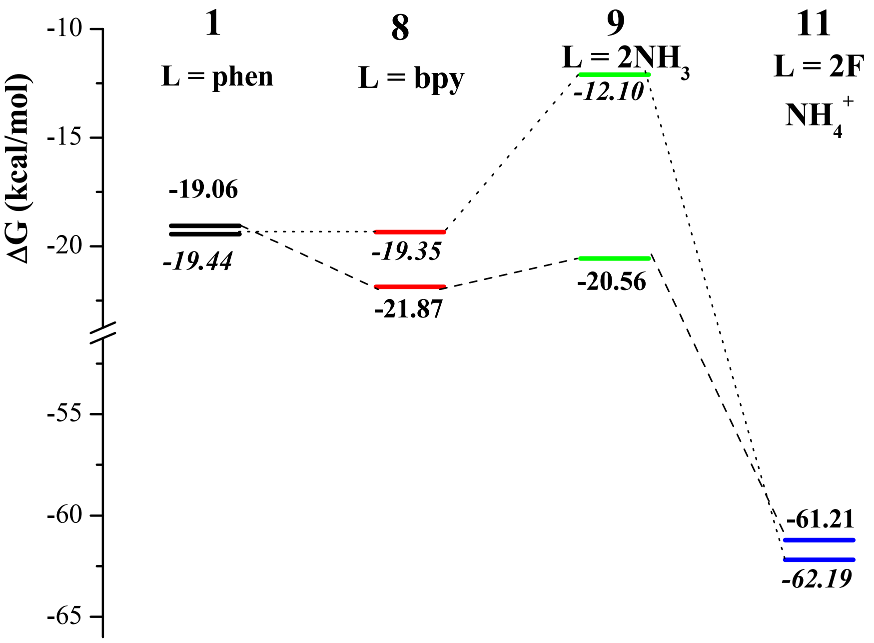

Figure S11. Free energies of formation reactions for bisuranyl complexes, $[(L)(UO_2)(\mu_2\text{-}F)(F)]_2$ (L = phen (**1**), bpy (**8**), and $2NH_3$ (**9**)) and $[NH_4]_4\cdot[(F)_2(UO_2)(\mu_2\text{-}F)(F)]_2$ (**11**), in the gas phase (connected by dot line) and aqueous solution (connected by dash line).

Table S1. Optimized geometry parameters and bond orders (in parentheses) of **2-4** in different electron-spin states. (Distance in angstrom and angle in degree)

	2 Np^{VI}			**3** Pu^{VI}		**4** U^{V}	
	Triplet	unrestr. Singlet	Quintuplet	Triplet	unrestr. Singlet	Triplet	unrestr. Singlet
An1=O	1.788 (2.36)	1.788 (2.36)	1.780 (2.33)	1.776 (2.33)	1.777 (2.33)	1.819 (2.36)	1.819 (2.36)
An1-F1	2.360 (0.52)	2.360 (0.52)	2.345 (0.53)	2.331 (0.55)	2.335 (0.54)	2.375 (0.54)	2.374 (0.54)
An1-F2	2.296 (0.57)	2.296 (0.57)	2.302 (0.55)	2.297 (0.56)	2.303 (0.55)	2.353 (0.54)	2.353 (0.54)
An1-F3	2.109 (1.14)	2.109 (1.14)	2.120 (1.12)	2.113 (1.12)	2.113 (1.12)	2.153 (1.09)	2.153 (1.09)
An1-N1	2.644 (0.31)	2.644 (0.31)	2.629 (0.31)	2.632 (0.31)	2.631 (0.31)	2.620 (0.40)	2.619 (0.40)
An1-N2	2.681 (0.32)	2.681 (0.30)	2.665 (0.30)	2.667 (0.30)	2.667 (0.30)	2.657 (0.38)	2.658 (0.38)
An1···An2	3.871 (0.06)	3.870 (0.06)	3.863 (0.06)	3.854 (0.08)	3.846 (0.07)	3.960 (0.00)	3.960 (0.00)
O=An=O	175.5	175.5	176.3	176.6	176.6	175.9	175.9
O-An1-An2	90.7	90.8	92.9	93.5/88.0	92.5	91.0	91.0
F1-An1-F2	67.5	67.6	67.5	67.9	67.9	66.2	66.2
An1-F1-An2	112.5	112.4	112.5	112.4	112.1	113.8	113.8
An1-F1-F2-An2	180.0	180.0	-178.1	-176.4	-178.1	180.0	180.0
ΔE (kcal/mol) [a]	0.00	-0.01	0.00	8.74	17.47	0.00	0.02

[a] The relative energy of complex in different electronic states, where the energy in the highest electron-spin state was assumed at 0.00 kcal/mol.

Table S2. Partial molecular orbital contributions (%) of **1**, **10** and **11** in the aqueous solution calculated at the TD-**B3LYP** level.

	1			**10**			**11**		
	Orb.s	Energy (eV)	Composition	Orb.s	Energy (eV)	Composition	Orb.s	Energy (eV)	Composition
LUMO+5	112a	-3.058	90% U(f_{z^3}, $f_{z(x^2-y^2)}$, f_{z^2x})	62a	-1.316	90% U($f_{y(3x^2-y^2)}$)	78a	-2.405	90% U($f_{x(x^2-3y^2)}$, $f_{z(x^2-y^2)}$))
LUMO+4	111a	-3.074	93% U(f_{xyz}, f_{z^2y}, $f_{y(3x^2-y^2)}$)	61a	-1.361	94% U($f_{y(3x^2-y^2)}$)	77a	-2.469	91% U($f_{x(x^2-3y^2)}$, $f_{z(x^2-y^2)}$, $f_{y(3x^2-y^2)}$)
LUMO+3	110a	-3.199	94% U(f_{xyz})	60a	-1.495	97% U($f_{z(x^2-y^2)}$)	76a	-2.524	90% U($f_{z(x^2-y^2)}$, $f_{x(x^2-3y^2)}$, f_{xyz})
LUMO+2	109a	-3.212	93% U(f_{z^2y}, $f_{y(3x^2-y^2)}$, f_{xyz})	59a	-1.511	94% U($f_{z(x^2-y^2)}$)	75a	-2.605	94% U(f_{xyz}, f_{z^2y}, $f_{x(x^2-3y^2)}$,)
LUMO+1	108a	-3.213	92% U(f_{z^3}, f_{z^2x}, $f_{z(x^2-y^2)}$)	58a	-1.561	96% U(f_{xyz})	74a	-2.627	94% U(f_{xyz}, $f_{z(x^2-y^2)}$, f_{z^2y})
LUMO	107a	-3.293	97% U(f_{z^2y}, $f_{y(3x^2-y^2)}$)	57a	-1.673	97% U(f_{xyz})	73a	-2.736	97% U(f_{xyz}, $f_{y(3x^2-y^2)}$, f_{xyz}, f_{z^2x})
HOMO	106a	-7.006	92% phen	56a	-7.232	42% U(f_{z^3}), 42% O(2p_z)	72a	-8.368	42% U(f_{z^3}, f_{z^2x}, f_{z^2y}), 40% O(2p_z)
HOMO-1	105a	-7.006	92% phen	55a	-7.301	41% U(f_{z^3}), 43% O(2p_z)	71a	-8.460	39% U(f_{z^2x}, f_{z^3}, f_{z^2y}), 42% O(2p_z)
HOMO-2	104a	-7.394	94% phen	54a	-7.952	97% [F(2*p*)+O(2*p*)]	70a	-9.058	79% [F(2*p*)+O(2*p*)]
HOMO-3	103a	-7.395	94% phen	53a	-7.958	88% [F(2*p*)+O(2*p*)]	69a	-9.230	78% [F(2*p*)+O(2*p*)]
HOMO-4	102a	-8.621	44% U($f_{y(3x^2-y^2)}$, f_{z^2y}), 34% O(2p_y)	52a	-7.959	91% [F(2*p*)+O(2*p*)]	68a	-9.287	86% [F(2*p*)+O(2*p*)]
HOMO-5	101a	-8.716	61% phen	51a	-7.983	95% [F(2*p*)+O(2*p*)]	67a	-9.293	83% [F(2*p*)+O(2*p*)]
HOMO-6	100a	-8.738	54% phen						
HOMO-7	99a	-8.754	37% U($f_{y(3x^2-y^2)}$, f_{z^2y}), 30% O(2p_y)						

Table S3. Partial molecular orbital contributions (%) of **1**, **10** and **11** in the aqueous solution calculated at the TD-**PBE** level.

	1			**10**			**11**		
	Orb.s	Energy (eV)	Composition	Orb.s	Energy (eV)	Composition	Orb.s	Energy (eV)	Composition
LUMO+5	112a	-4.053	93% U($f_{xyz}, f_{z^{2}y}, f_{y(3x^{2}-y^{2})}$)	62a	-2.747	88% U($f_{y(3x^{2}-y^{2})}$)	78a	-3.969	88% U($f_{x(x^{2}-3y^{2})}, f_{z(x^{2}-y^{2})}, f_{y(3x^{2}-y^{2})}$)
LUMO+4	111a	-4.100	89% U($f_{z^{3}}, f_{z(x^{2}-y^{2})}, f_{z^{2}x}$)	61a	-2.801	90% U($f_{y(3x^{2}-y^{2})}$)	77a	-4.014	91% U($f_{z(x^{2}-y^{2})}, f_{x(x^{2}-3y^{2})}, f_{z^{2}x}$)
LUMO+3	110a	-4.172	94% U(f_{xyz})	60a	-2.917	94% U($f_{z(x^{2}-y^{2})}$)	76a	-4.064	90% U($f_{x(x^{2}-3y^{2})}, f_{z(x^{2}-y^{2})}, f_{xyz}$)
LUMO+2	109a	-4.221	97% U($f_{z^{2}y}, f_{y(3x^{2}-y^{2})}, f_{xyz}$)	59a	-2.918	93% U($f_{z(x^{2}-y^{2})}$)	75a	-4.116	92% U($f_{x(x^{2}-3y^{2})}, f_{z(x^{2}-y^{2})}, f_{z^{2}y}$)
LUMO+1	108a	-4.239	93% U($f_{z^{3}}, f_{z(x^{2}-y^{2})}, f_{z^{2}x}$)	58a	-2.99	95% U(f_{xyz})	74a	-4.147	94% U($f_{xyz}, f_{z(x^{2}-y^{2})}, f_{z^{2}y}$)
LUMO	107a	-4.297	97% U($f_{z^{2}y}, f_{y(3x^{2}-y^{2})}$)	57a	-3.095	98% U(f_{xyz})	73a	-4.253	97% U($f_{xyz}, f_{y(3x^{2}-y^{2})}, f_{xyz}, f_{z^{2}x}$)
HOMO	106a	-6.384	90% phen	56a	-5.763	43% U($f_{z^{3}}$), 38% O($2p_{z}$)	72a	-6.955	43% U($f_{z^{2}x}, f_{z^{3}}, f_{z^{2}y}$), 36% O($2p_{z}$)
HOMO-1	105a	-6.384	90% phen	55a	-5.838	33% U($f_{z^{3}}$), 35% O($2p_{z}$)	71a	-7.049	44% U($f_{z^{2}x}, f_{z^{3}}, f_{z^{2}y}$), 36% O($2p_{z}$)
HOMO-2	104a	-6.766	92% phen	54a	-6.369	99% [F($2p$)+O($2p$)]	70a	-7.647	88% [F($2p$)+O($2p$)]
HOMO-3	103a	-6.767	92% phen	53a	-6.433	100% [F($2p$)+O($2p$)]	69a	-7.793	88% [F($2p$)+O($2p$)]
HOMO-4	102a	-7.026	44% U($f_{y(3x^{2}-y^{2})}, f_{z^{2}y}$), 35% O($2p_{y}$)	52a	-6.44	96% [F($2p$)+O($2p$)]	68a	-7.823	85% [F($2p$)+O($2p$)]
HOMO-5	101a	-7.183	45% U($f_{y(3x^{2}-y^{2})}, f_{z^{2}y}$), 35% O($2p_{y}$)	51a	-6.443	94% [F($2p$)+O($2p$)]	67a	-7.832	89% [F($2p$)+O($2p$)]

Table S4. Calculated absorptions of complexes **1** in the aqueous solution at the TD-B3LYP/TZP/ZORA/COSMO level.

Compl.s	States	λ (nm) [a]	E (eV) [a]	E (cm^{-1}) [a]	f [b]	Configurations	Weight > 0.2
1	S_1	400	3.10	25000	0.056	106a→107a	0.4645
	S_5	387	3.20	25840	0.025	106a→110a	0.4832
	S_8	366	3.39	27322	0.003	105a→109a	0.3891
						106a→107a	0.2746
	S_{14}	357	3.48	28011	0.157	103a→107a	0.5194
						103a→109a	0.2864
	S_{16}	354	3.50	28249	0.057	105a→111a	0.4660
	S_{18}	353	3.51	28329	0.017	102a→109a	0.2824
						99a→107a	0.2248
	S_{23}	347	3.58	28818	0.110	104a→110a	0.6377
						104a→111a	0.2446
	S_{24}	346	3.58	28902	0.107	103a→110a	0.6375
						103a→111a	0.2546
	S_{26}	341	3.63	29326	0.092	102a→111a	0.4210
						99a→110a	0.3564
	S_{31}	330	3.75	30303	0.006	103a→109a	0.5846
						103a→107a	0.3237
	S_{35}	321	3.87	31153	1.000	105a→116a	0.3769
						106a→115a	0.3542
	S_{37}	320	3.87	31250	0.174	103a→111a	0.5752
						103a→110a	0.2197
11	S_5	310	3.99	32258	0.026	71a→75a	0.4250
						71a→74a	0.2824
	S_6	309	4.02	32362	0.016	72a→76a	0.3961
						72a→77a	0.3416
	S_9	257	4.83	38911	0.032	70a→73a	0.4182
	S_{24}	240	5.16	41667	0.172	72a→76a	0.3006
						72a→77a	0.2669
	S_{25}	238	5.22	42017	0.411	67a→73a	0.2154
	S_{27}	237	5.24	42194	0.029	70a→78a	0.2753
	S_{29}	235	5.27	42553	0.264	71a→77a	0.3048
						71a→76a	0.2909
	S_{32}	233	5.32	42918	0.106	69a→78a	0.2012
	S_{35}	231	5.38	43290	0.019	71a→78a	0.5301
						70a→78a	0.2360
	S_{37}	228	5.43	43860	1.000	68a→76a	0.2583
						68a→77a	0.2142

[a] Calculated absorption spectra in nm, eV and cm^{-1}. [b] Oscillator strength was normalized for convenient comparison.